Six similar sequential ruptures of the San Andreas fault, Carrizo Plain, California

Jing Liu
Yann Klinger
Division of Geological and Planetary Sciences, California Institute of Technology, Pasadena, California 91125, USA, and Laboratoire de Tectonique, Institut de Physique du Globe de Paris, 4 place Jussieu, 75252 Paris cedex 05, France
Kerry Sieh*
Division of Geological and Planetary Sciences, California Institute of Technology, Pasadena, California 91125, USA
Charles Rubin
Department of Geological Sciences, Central Washington University, Ellensburg, Washington 98926, USA

ABSTRACT

We document the precise sizes, but not the dates, of the six latest offsets across the San Andreas fault at Wallace Creek, California. Three and perhaps four of these, including the latest in 1857, show dextral offset of 7.5–8 m. The third and fourth offsets, however, are just 1.4 and 5.2 m. The predominance of similar offsets for the latest six events suggests that the fundamental properties of the fault system that control slip size do not vary greatly from event to event. The large offsets imply that ruptures involving this site are typically more than 200 km long.

Keywords: San Andreas, fault, paleoseismology, earthquake, rupture.

INTRODUCTION

Concepts and models of repeating fault rupture are tenuous, because there are few data to test them. Some advocate sequences that are highly regular in time or rupture parameters (e.g., Reid, 1910; Tse and Rice, 1986; Schwartz and Coppersmith, 1984; Lapusta et al., 2000). Others predict irregular behavior, where rupture parameters and frequency range over orders of magnitude (e.g., Bak and Teng, 1989; Carlson and Langer, 1989; Ben-Zion, 1996; Shaw and Rice, 2000). Probabilistic earthquake forecasts usually assume nearly periodic identical ruptures (e.g., Working Group on California Earthquake Probabilities, 2002), although combinations with other behaviors have also been attempted (e.g., Frankel et al., 1996; Giardini, 1999).

Acquiring data that constrain physical models is difficult, because repose times between large ruptures of a single fault are hundreds to thousands of years, far longer than observational histories. Paleoseismic methods, however, can produce records of fault slip through numerous earthquake cycles (McCalpin, 1996; Yeats et al., 1997). Some paleoseismic data show that slip at a given location is similar from one earthquake to the next (Sieh, 1996; Klinger et al., 2003; Streig et al., 2004). However, well-constrained paleoseismic data sets rarely contain more than two sequential ruptures. Longer records are usually based on in-

direct evidence or have large uncertainties in slip sizes (e.g., Schwartz and Coppersmith, 1984; Sieh, 1984; Pantosti et al., 1996).

Better long records would narrow the wide range of predicted behaviors. Thus our goal in this study was to document precisely many sequential offsets from a single fault site. We were half successful; we recovered a precise record of offsets for six sequential ruptures, but we could not determine precisely their dates.

DESCRIPTION OF THE SITE AND METHODS

The San Andreas fault in the Carrizo Plain is unusually simple and well expressed. Wallace (1968) first used small offset gullies here to estimate slip of the great 1857 and earlier earthquakes. Later work (Sieh, 1978) suggested that the latest three ruptures just southeast of Wallace Creek (Fig. 1A) were 9.5–12.5 m. Excavations by Grant and Sieh (1993) nearby yielded an 1857 offset of ~7 m. At Wallace Creek, Sieh and Jahns (1984) determined a late Holocene slip rate of ~34 mm/yr and speculated that at this rate, offsets of ~10 m would recur every ~300 yr.

At our Wallace Creek paleoseismic site (Fig. 1A), gullies downstream from the fault are dextrally offset from a solitary upstream channel (Fig. 1B). The shape of the youngest gully suggests ~7–10 m of slip in 1857 (Sieh, 1978; Grant and Sieh, 1993). Older offset gullies, farther northwest, are more subdued but still visible. Slope wash from the scarp par-

tially buries these, so their precise geometry near the fault is obscure.

To determine exactly the number, size, and sequence of the dextral offsets, we exposed the subsurface shape and stratigraphy of the channels (Liu, 2003). We began by hand-digging narrow trenches across the gullies, 4–5 m from and parallel to the fault. After precisely surveying and mapping these trench walls, we cut into the wall closer to the fault in increments of 20 to 60 cm, progressively mapping each new exposure. In this manner, we carefully followed each potential piercing line into the fault zone. These three-dimensional excavations enabled us to reconstruct channel and fault geometries with errors of just a few centimeters.

EVIDENCE FOR BURIED OFFSETS

The excavations revealed 12 buried channels on the downstream side of the fault, beneath the four topographically obvious channels (Fig. 2A). Most of these were solitary channels with repeated scours and fills. The deeper parts of a channel commonly had sharp walls, made clear by the contrast of internal and external strata. Beds within a channel were commonly loose, pebbly, fluvial sand and colluvial debris, whereas strata cut by a channel typically were harder, massive, poorly sorted gravelly sand and silt. Channel fills were generally looser and darker than material outside the channels. Except for channels c, h, and j, the downstream channels intersect the
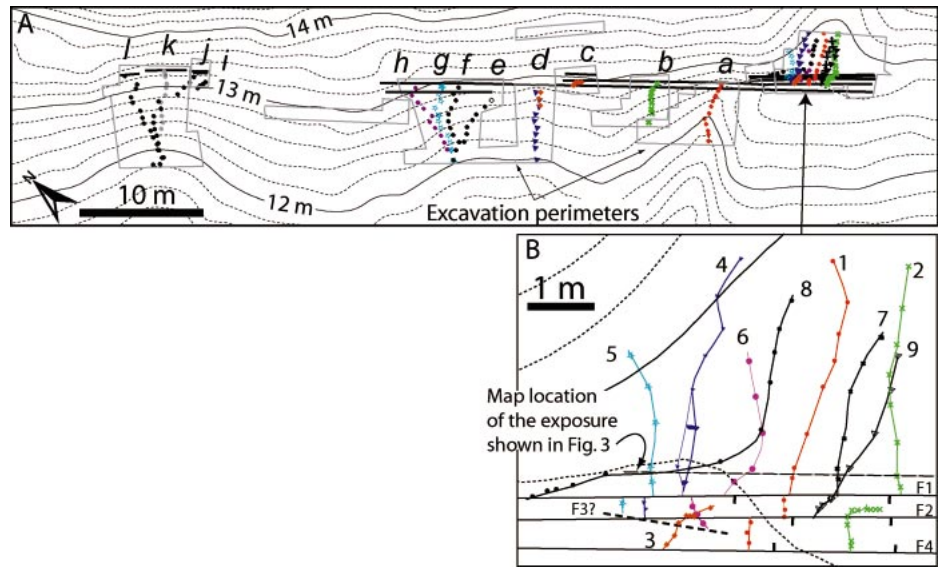
*Corresponding author. E-mail: sieh@gps.caltech.edu.
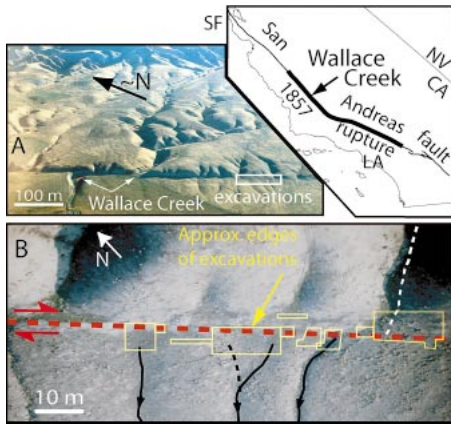
Figure 1. Two oblique aerial views of paleo-seismic site. A: Small drainages few hundred of meters southeast of Wallace Creek offer unusual opportunity to determine offset size during past ruptures. Photo by P. Tapponnier. B: Four channels downstream from fault appear to be offset from single upstream channel.

Figure 2. Map views of buried channels at site. Each colored symbol represents position of channel thalweg mapped and surveyed in excavation wall. Letters denote downstream channels and numbers represent upstream channels. Colors indicate correlations across fault. Gray and black lines are channels with no known correlatives across fault. Thick black lines indicate surface projections of fault traces. Ticks on faults F1, F2 and F4 show downthrown side.

fault at high angles. Channels e and i do not intersect the fault.

Upstream exposures revealed nine nested channels (Fig. 3). Several channels contain distinctive laminated beds of well-sorted fines, deposited as suspended load from water ponded behind shutter ridges after large offsets. Most of these channels intersect the fault at a high angle (Fig. 2B). The internal stratigraphy and shape of both upstream and downstream channel segments constrain fault rupture and warping to a narrow zone (Fig. 2). Distortion in channel shape and warping of channels due to shearing appear only within tens of centimeters of the fault traces.

We can match the youngest five channel pairs across the fault (Fig. 4). Correlation of the sixth pair is less certain. Matches are based on (1) crosscutting relationships in the upstream exposures, (2) shapes and internal stratigraphy of the channels, and (3) angles at which channels intersect the fault. Radiocarbon analyses of detrital charcoal show that all six matched channels formed in the past ~1 k.y., and that all the uncorrelated channels are at least 2500 yr old (Liu, 2003). Ranges of ages within individual channels are as great as 1 k.y., however, so it is clear that significant reworking of carbon has occurred. Thus, individual channel ages are poorly constrained.

Crosscutting relations of clustered channels (e.g., e, f, g, and h) allow determination of relative ages of some downstream channels. The relative ages of most of the upstream channels are clear from their crosscutting relations (Fig. 3). However, some of these relations have been obliterated by erosion. For example, the stratigraphic relation of channel 2 to channels 4, 5, and 6 is uncertain, due to incision of younger channel 1. Fortunately,

matching of channel shapes and internal stratigraphy with channels across the fault zone resolves such ambiguities in relative age. Thus, the evidence is strong for the correlation of upstream channels 1, 2, 3, 4, and 5 with downstream channels a, b, c, d, and g, respectively. The match of channels 6 and h is less certain, because younger channels have eroded much of channel 6. The correlation of 6 and h is based upon channel size, fill, and the acute angle of intersection of both channels with the fault. Channel 6 is the only upstream channel to trend southward near the main fault, and so its downstream equivalent should also trend southward away from the fault.
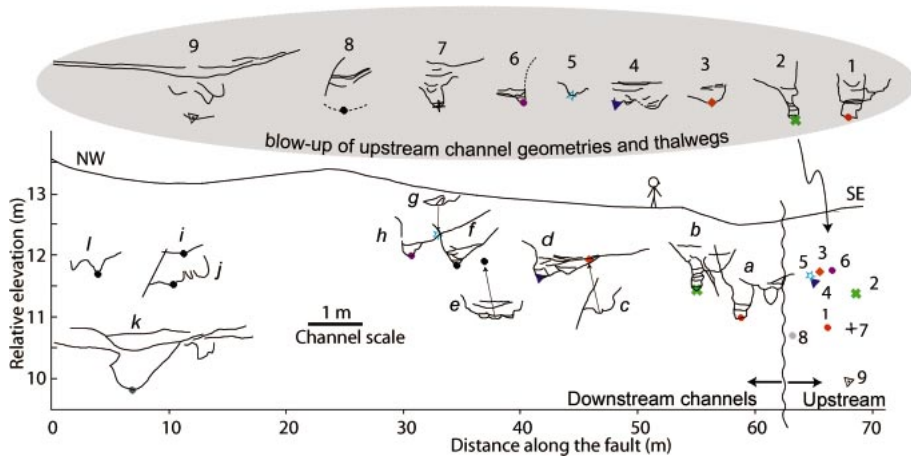
Upstream channels 7, 8, and 9 and downstream channels e, f, i, j, k, and l have no correlatives within the excavated volumes. Downstream correlatives of channels 7, 8, and 9 likely exist farther to the northwest, and upstream correlatives of channels e, f, i, j, k, and l probably reside farther southeast. Sparse radiocarbon ages of ≥2500 yr on detrital charcoal within these older channels support this inference (Liu, 2003).

OFFSET SEQUENCE

Matching thalwegs and other channel features across the fault allows us to recover their horizontal and vertical offsets, because we can
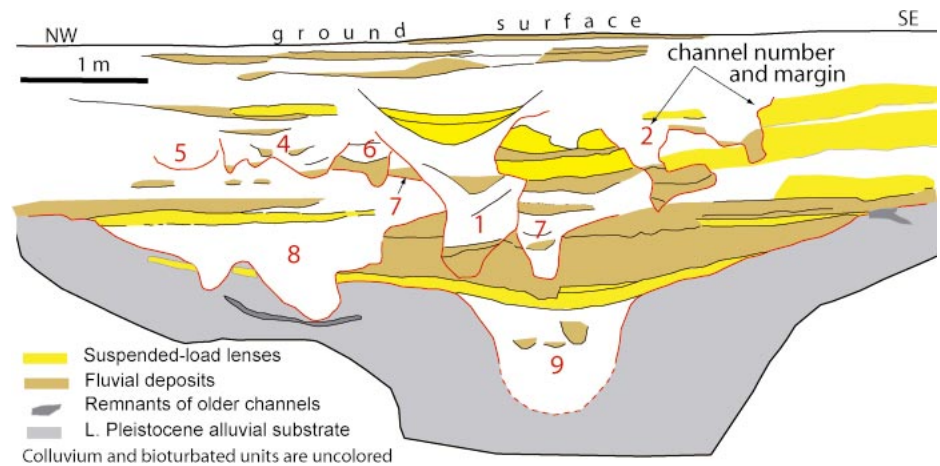
Figure 3. Simplified map of wall of upstream excavation shows eight of nine nested channels. Suspended-load deposits attest to temporary ponding behind shutter ridges after large dextral offsets. Channel 3 does not extend upstream as far as cross section. Many channel strata have been bioturbated, but enough fluvial stratigraphy remains, especially in lower portions of channels, to enable correlation of units across fault.

Figure 4. Relative locations of downstream and upstream channel bottoms (thalwegs) at their intersection with fault, projected onto vertical plane parallel to fault. Wavy vertical line separates domains of upstream and downstream channels. Downstream channel shapes and strata appear at enlarged scale atop their thalwegs. Thalwegs of upstream channels are nested close together, so details of their shapes and strata appear within shaded ellipse above vertical section. Figure 3 shows stratigraphic relations of these upstream channels. Colors show correlative upstream and downstream thalwegs.

reconstruct channel geometries in three dimensions (Fig. 5). For example, the size of event WC1 (7.9 ± 0.1 m) is the dextral offset of channel pair 1 and a. The vertical offset is only a few centimeters, southwest side up. The size of penultimate event WC2 (7.6 ± 0.4 m) is the offset of channel pair 2 and b minus the offset of pair 1 and a. The vertical offset is ~10–15 cm, northeast side up. Offset WC6 is the only equivocal one. The acuteness of the intersection angles allows that the offset could be substantially >5.4 ± 0.6 m.

Altogether, ~36 m of dextral slip has accumulated in six discrete episodes. The size of the offsets, from oldest (WC6) to youngest (WC1), is ≥5.4, 8.0, 1.4, 5.2, 7.6, and 7.9 m (Fig. 5). Uncertainty is commonly a few tens of centimeters or less, because of the precision of the surveying and the sharpness of the stratigraphic piercing points. Cumulative vertical offset is nil, although for individual offsets the vertical component ranges as high as ~30 cm.

None of these six youngest offsets likely represents more than one rupture event. Frequent alluvial cuts and fills have resulted in

two or more subordinate cuts and fills within each of the channels. We would expect deflections of subordinate cuts and fills near the fault if offset had occurred soon after their formation. The lack of such deflections suggests that the offsets represent single events.

The gully occupied by channel pairs 4 and d and 3 and c underwent a clear postoffset deflection (Liu, 2003). The deeper, older parts of the gully are segments 4 and d (Fig. 2A). These segments intersect the fault at nearly right angles and thus appear to have been normal to the fault prior to offset. Channel c, higher in the fill sequence, trends southeastward near the fault. Another piece of channel c appears within the fault zone still farther southeast, extending at a very acute angle to the fault zone. Its correlative is upstream channel 3, which strikes at an acute angle to the fault trace and does not continue far upstream. The relations of channel pairs 4 and d and 3 and c thus demonstrate that a channel was offset ~1.4 m, then reoccupied by a new, deflected channel, which was later offset an additional 5.2 m (Liu, 2003). This example of subtleties in site stratigraphy suggests that if

any of the other discrete offsets represented more than one event, each would be recognizable in the internal stratigraphy of the channels.

Furthermore, the abrupt termination of channel walls and channel stratigraphy at the fault strongly suggests that the offsets occurred suddenly. The lack of dog-leg deflections in channel stratigraphy (other than in the case of channel pair 3 and c) and the narrowness of the channels support our analysis that the latest 36 m of dextral offset have accumulated in just six sudden events (Liu, 2003). The channel shapes and their infills might not allow discrimination of events that occurred just a few days or months apart.

IMPLICATIONS

The Wallace Creek paleoseismic site has yielded a long and precise, albeit poorly dated, sequence of serial fault ruptures. Three and possibly four of the six offsets are between 7.5 and 8 m, and ~95% of recent slip has accrued in 5.2–8.0 m increments. This means that slip sizes are much closer to regular than to stochastic (Liu, 2003), and that those properties of the fault system that control slip size vary little from event to event. Furthermore, the accrual of offset predominantly in increments of 5.2–8 m supports the concept of the earthquake cycle, wherein strain is slowly stored and then quickly released during large, similar dislocations (Reid, 1910; Tse and Rice, 1986; Lapusta et al., 2000).

Our data do not support models that produce great complexity of fault slip, including those that generate power-law frequency-size distributions of seismicity on single faults (e.g., Shaw and Rice, 2000). Such models predict variability in offset values over orders of magnitude. Physical models that produce more uniform rupture sequences, with populations of slip sizes like those seen at our site, use smoothing parameters and assume rupture patches with uniform frictional properties along strike, large critical-patch size for rupture preparation, or a high degree of geometrical or material regularity within fault zones
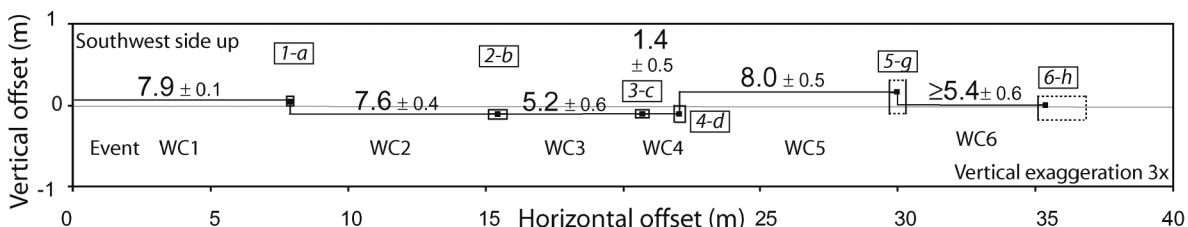
Figure 5. Horizontal and vertical offsets of channel pairs derived from data in Figure 4. Letter-number pairs in boxes are correlated channels. Uncertainties in horizontal and vertical offset of each pair appear as small black rectangle (Liu, 2003). Amount of dextral offset for six discrete ruptures (WC1–WC6) ranges from 1.4 to 8.0 m, but at least three and perhaps four are between 7.5 and 8.0 m. Vertical components of slip are small fractions of dextral offset, and their sense varies through sequence.
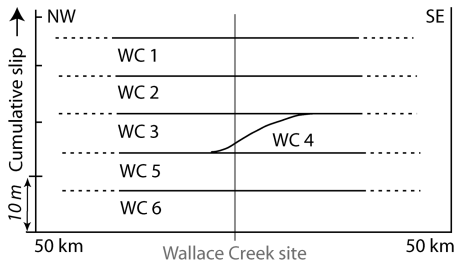
Figure 6. Two smaller events in mid-sequence might represent two overlapping ruptures in which tail of event WC4 tapers to northwest and tail of later event WC3 tapers to southeast.

(e.g., Rice and Ben-Zion, 1996; Ben-Zion, 1996; Ward, 1997).

The presence of 1.4 m and 5.2 m events in the middle of the sequence show that behavior is not strictly uniform. Promoters of characteristic-slip models might suggest that the consecutive 1.4 and 5.2 m offsets represent two closely timed ruptures that overlapped in the vicinity of Wallace Creek (Fig. 6). They might note that these add up to nearly 7 m, a common slip value at the site. This interpretation is inconsistent, however, with theoretical models that produce complete ruptures of smooth fault planes (Rice and Ben-Zion, 1996). Perhaps this is not a major hindrance, because these theoretical results are at odds with observations of large ruptures terminating in the middle of planar faults (e.g., Sharp et al., 1982; Sieh et al., 1993).

The large size of most offsets at Wallace Creek implies very long associated rupture lengths. Biasi et al. (2004) showed, from a probabilistic treatment of well-mapped modern fault ruptures, that even offsets of 6 m likely reflect rupture extents >200 km and earthquake magnitudes (M_w) > 7.8. Thus it is likely that the larger ruptures extended southeastward much of the distance to Los Angeles.

REFERENCES CITED
Bak, P., and Tang, C., 1989, Earthquakes as a self-organized critical phenomenon: Journal of Geophysical Research, v. 94, p. 15,635–15,637.

Ben-Zion, Y., 1996, Stress, slip, and earthquakes in models of complex single-fault systems incorporating brittle and creep deformations: Journal of Geophysical Research, v. 101, p. 5677–5706.

Biasi, G., Weldon, R., Fumal, T., and Scharer, K., 2004, Using point displacement measurements to constrain the rupture history of the southern San Andreas fault: Seismological Research Letters, v. 75, no. 2, p. 254.

Carlson, J., and Langer, J., 1989, Properties of earthquakes generated by fault dynamics: Physical Review Letters, v. 62, p. 2632–2635.

Frankel, A., Mueller, C., Barnhard, T., Perkins, D., Leyendecker, E., Dickman, N., Hanson, S., and Hopper, M., 1996, National seismic hazard maps: U.S. Geological Survey Open-File Report 96-532, 100 p., http://eqhazmaps.usgs.gov/html/canvmap.html (accessed April 2004).

Giardini, D., ed., 1999, Global Seismic Hazard Assessment Program (GSHAP) 1992–1999: Annali di Geofisica, v. 42, p. 957–974.

Grant, L., and Sieh, K., 1993, Stratigraphic evidence for 7 meters of dextral slip on the San Andreas fault during the 1857 earthquake in the Carrizo Plain: Seismological Society of America Bulletin, v. 83, p. 619–635.

Klinger, Y., Sieh, K., Altunel, E., Akoglu, A., Barka, A., Dawson, T., Gonzalez, T., Meltzner, A., and Rockwell, T., 2003, Paleoseismic evidence of characteristic slip on the western segment of the North Anatolian fault, Turkey: Seismological Society of America Bulletin, v. 93, p. 2317–2332.

Lapusta, N., Rice, J., Ben-Zion, Y., and Zheng, G., 2000, Elastodynamic analysis for slow tectonic loading with spontaneous rupture episodes on faults with rate- and state-dependent friction: Journal of Geophysical Research, v. 105, p. 23,765–23,789.

Liu, J., 2003, Slip behavior of the San Andreas fault through several earthquake cycles [Ph.D. thesis]: Pasadena, California Institute of Technology, http://resolver.caltech.edu/CaltechETD:etd-05272003-095416.

McCalpin, J., 1996, Paleoseismology: Cambridge, Cambridge University Press, 588 p.

Pantosti, D., Collier, R., D'Addezio, G., Masana, E., and Sakellariou, D., 1996, Direct geological evidence for prior earthquakes on the 1981 Corinth fault (central Greece): Geophysical Research Letters, v. 23, p. 3795–3798.

Reid, H., 1910, The mechanics of the earthquake: The California earthquake of April 18, 1906: Report of the State Earthquake Investigation Commission, Volume 2: Washington, D.C., Carnegie Institution of Washington, 192 p.

Rice, J., and Ben-Zion, Y., 1996, Slip complexity in earthquake fault models: National Academy of Sciences Proceedings, v. 93, p. 3811–3818.

Schwartz, D., and Coppersmith, K., 1984, Fault behavior and characteristic earthquakes: Examples from the Wasatch and San Andreas fault zones: Journal of Geophysical Research, v. 89, p. 5681–5698.

Sharp, R., Lienkaemper, J., Bonilla, M., Burke, D., Cox, B., Herd, D., Miller, D., Morton, D., Ponti, D., Rymer, M., Tinsley, J., Yount, J.,

Kahle, J., Hart, E., and Sieh, K., 1982, Surface faulting in the central Imperial Valley, *in* The Imperial Valley, California, earthquake of October 15, 1979: U.S. Geological Survey Professional Paper 1254, p. 119–144.

Shaw, B., and Rice, J., 2000, Existence of continuum complexity in the elastodynamics of repeated fault ruptures: Journal of Geophysical Research, v. 105, p. 791–823.

Sieh, K., 1978, Slip along the San Andreas fault associated with the great 1857 earthquake: Seismological Society of America Bulletin, v. 68, p. 1421–1448.

Sieh, K., 1984, Lateral offsets and revised dates of large prehistoric earthquakes at Pallett Creek, southern California: Journal of Geophysical Research, v. 89, p. 7641–7670.

Sieh, K., 1996, The repetition of large-earthquake ruptures: National Academy of Sciences Proceedings, v. 93, p. 3764–3771.

Sieh, K., and Jahns, R., 1984, Holocene activity of the San Andreas fault at Wallace Creek, California: Geological Society of America Bulletin, v. 95, p. 883–896.

Sieh, K., Jones, L., Hauksson, E., Hudnut, K., Eberhart-Phillips, D., Heaton, T., Hough, S., Hutton, K., Kanamori, H., Lilje, A., Lindvall, S., McGill, S., Mori, J., Rubin, C., Spotila, J., Stock, J., Thio, H., Treiman, J., Wernicke, B., and Zachariasen, J., 1993, Near-field investigations of the Landers earthquake sequence, April to July, 1992: Science, v. 260, p. 171–176.

Streig, A., Rubin, C., Chen, W., Chen, Y., Lee, L., Thompson, S., and Lu, S., 2004, Evidence for prehistoric coseismic folding along the Tsaotun segment of the Chelungpu fault near Nan-Tou, Taiwan: Seismic hazard along active fold scarps: Journal of Geophysical Research (in press).

Tse, S., and Rice, J., 1986, Crustal earthquake instability in relation to the depth variation of frictional slip properties: Journal of Geophysical Research, v. 91, p. 9452–9472.

Wallace, R., 1968, Notes on stream channels offset by the San Andreas fault, southern Coast Ranges, California: Conference on Geologic Problems of the San Andreas Fault System, Proceedings: Stanford, California, Stanford University Publications in the Geological Sciences 11, p. 6–21.

Ward, S., 1997, Dogtails versus rainbows: Synthetic earthquake rupture models as an aid in interpreting geological data: Seismological Society of America Bulletin, v. 87, p. 1422–1441.

Working Group on California Earthquake Probabilities, 2002, Summary of earthquake probabilities in the San Francisco Bay region: 2003–2032: http://quake.usgs.gov/research/seismology/wg02/summary/ (accessed April 2004).

Yeats, R., Sieh, K., and Allen, C., 1997, The geology of earthquakes: New York, Oxford University Press, 568 p.